Antiviral Research 100 (2013) 337–345

Contents lists available at ScienceDirect

Antiviral Research

journal homepage: www.elsevier.com/locate/antiviral

Single-stranded DNA aptamer that specifically binds to the influenza virus NS1 protein suppresses interferon antagonism

Hye-Min Woo [a,1], Ki-Sun Kim [a,1], Jin-Moo Lee [a], Hee-Sup Shim [a], Seong-Je Cho [a], Won-Kyu Lee [a], Hyuk Wan Ko [b], Young-Sam Keum [b], Soo-Youl Kim [c], Prabuddha Pathinayake [d], Chul-Joong Kim [d], Yong-Joo Jeong [a,*]

[a] Department of Bio and Nanochemistry, Kookmin University, Seoul 136-702, Republic of Korea
[b] College of Pharmacy, Dongguk University, Goyang, Gyeonggi-do 410-820, Republic of Korea
[c] Cancer Cell & Molecular Biology Branch, Division of Cancer Biology, Research Institute, National Cancer Center, Goyang 410-769, Republic of Korea
[d] College of Veterinary Medicine, Chungnam National University, Daejeon 305-764, Republic of Korea

ARTICLE INFO

Article history:
Received 7 February 2013
Revised 6 September 2013
Accepted 8 September 2013
Available online 19 September 2013

Keywords:
Influenza virus
NS1
Aptamer
Interferon
G-quadruplex

ABSTRACT

Non-structural protein 1 (NS1) of the influenza A virus (IAV) inhibits the host's innate immune response by suppressing the induction of interferons (IFNs). Therefore, blocking NS1 activity can be a potential strategy in the development of antiviral agents against IAV infection. In the present study, we selected a single-stranded DNA aptamer specific to the IAV NS1 protein after 15 cycles of systematic evolution of ligands by exponential enrichment (SELEX) procedure and examined the ability of the selected aptamer to inhibit the function of NS1. The selected aptamer binds to NS1 with a K_d of 18.91 ± 3.95 nM and RNA binding domain of NS1 is determined to be critical for the aptamer binding. The aptamer has a G-rich sequence in the random sequence region and forms a G-quadruplex structure. The localization of the aptamer bound to NS1 in cells was determined by confocal images, and flow cytometry analysis further demonstrated that the selected aptamer binds specifically to NS1. In addition, luciferase reporter gene assay, quantitative RT-PCR, and enzyme-linked immunosorbent assay (ELISA) experiments demonstrated that the selected aptamer had the ability to induce IFN-β by suppressing the function of NS1. Importantly, we also found that the selected aptamer was able to inhibit the viral replication without affecting cell viability. These results indicate that the selected ssDNA aptamer has strong potential to be further developed as a therapeutic agent against IAV.

1. Introduction

Influenza viruses cause respiratory disease and continue to be one of the largest global threats to human health. The viruses belong to the family *Orthomyxoviridae* and are further divided into subtypes depending on the types of hemagglutinin and neuraminidase present. They are enveloped viruses that contain single-stranded negative-sense RNA consisting of 8 segments.

To prevent viral proliferation, the host cells initiate a strong antiviral response (Randall and Goodbourn, 2008), such as the innate immune response. The innate immune response is the front line of the host's defense system against invading pathogens. It recognizes the conserved motif or pathogen-associated molecule patterns (PAMPs) of incoming microorganisms by binding to pattern-recognition receptors such as the Toll-like receptors (TLRs) (Kaisho and Akira, 2006). RIG-I-like receptors (RLRs), another innate immune system of hosts, also play an important role by recognizing the intracellular double-stranded (ds) RNA or 5′-triphosphate RNA, molecular products of many RNA viruses during infection (Yoneyama et al., 2004). The major role of innate immunity, including both TLRs and RLRs, is the production of interferons (IFNs), which are antiviral cytokines inducing a range of antiviral responses.

Influenza viruses have evolved several strategies to circumvent the host's innate immune response (Grimm et al., 2007; Kurokawa et al., 1999). One of the most common strategies adopted by influenza viruses for evading their host's innate immune response is dependent on the function of the influenza non-structural protein 1 (NS1) (Egorov et al., 1998; Garcia-Sastre et al., 1998; Kochs et al., 2007). NS1 is a multifunctional protein, ~230 amino acids in length, and is known to participate in protein–protein and protein–RNA interactions during viral infection (Suarez and Perdue, 1998). However, the major role of NS1 is to antagonize IFN production leading to the inhibition of the host's innate immunity (Don-

* Corresponding author. Address: Department of Bio and Nanochemistry, Kookmin University, 77 Jeongneung-Ro, Seongbuk-Gu, Seoul 136-702, Republic of Korea. Tel.: +82 2 910 5454; fax: +82 2 910 4415.
E-mail address: jeongyj@kookmin.ac.kr (Y.-J. Jeong).
[1] These two authors contributed equally to this work.

0166-3542/$ - see front matter © 2013 Elsevier B.V. All rights reserved.
http://dx.doi.org/10.1016/j.antiviral.2013.09.004

elan et al., 2003; Talon et al., 2000a; Wang et al., 2000). Since the emergence of these intriguing findings related to the inhibitory role of NS1 in IFN production, many attempts have been made to elucidate the molecular mechanism by which NS1 represses IFN expression in the process of viral infection. One possibility involves the sequestration of viral RNA by NS1, which results in the inhibition of access to viral RNA sensors such as RIG-I (Talon et al., 2000a). Direct interaction of NS1 with RIG-I, which suppresses the RIG-I pathway and eventually inhibits IFN production, has also been suggested to be a potential mechanism (Guo et al., 2007; Pichlmair et al., 2006). In addition, NS1 has also been shown to specifically inhibit TRIM25-mediated RIG-I caspase recruitment domain (CARD) ubiquitination, leading to the suppression of the RIG-I pathway (Gack et al., 2009). However, the precise mechanism by which NS1 antagonizes IFN production remains unknown.

Considering the importance of NS1 during viral infection, targeting NS1 offers a very attractive potential therapeutic measure for anti-influenza drug development. This involves the inhibition of the interaction between NS1 and host factors or viral RNA in order to restore the production of IFN. Twu et al. described the peptide-mediated inhibition of NS1-cleavage and polyadenylation specificity factor (CPSF) 30 interaction (Twu et al., 2006), but this attempt was hindered by virus mutation and drug resistance.

Recently, nucleic acid aptamers have been put forward for use as specific ligands for therapeutic agents against many human diseases due to their inhibitory ability and target specificity (Bunka et al., 2010). Because the binding affinities of selected aptamers have been shown to be comparable to those of corresponding antibodies, aptamers have been referred to as 'chemical antibodies' (Brody and Gold, 2000). Their ability to form tertiary structures enables selected aptamers to be potential candidates for the development of drugs against various human diseases (Vo et al., 2003).

In this study, we identified and described a single-stranded (ss) DNA aptamer specific to influenza NS1 protein. The selected ssDNA aptamer shows specific binding to NS1 *in vitro* and in cells. Interestingly, the aptamer induced IFN production by suppressing NS1 and inhibited viral replication, which suggests that the selected ssDNA aptamer can be developed as an antiviral agent after further investigation.

2. Materials and methods

2.1. SELEX procedure

The DNA library, composed of 2 primer regions and a 45-base random region, was prepared, and ssDNAs were generated as described previously (Cho et al., 2011). *In vitro* selection of ssDNA aptamers specific to the GST-tagged NS1 protein was performed as described previously (Cheng et al., 2008; Cho et al., 2011) with slight modifications. The synthetic ssDNA library was denatured by heating at 95 °C for 10 min, and immediately annealed on ice for 10 min. Then, 5 μg of the DNA library was incubated with 100 μL of glutathione agarose beads in 100 μL of binding buffer (50 mM Tris/Cl (pH 8.0), 150 mM NaCl, 1.5 mM $MgCl_2$, 2 mM DTT and 1% (w/v) BSA) for 30 min at room temperature with occasional shaking. Nonspecific bead-bound DNA was precipitated and discarded. The pre-cleared supernatant was collected and incubated with 2 μg of GST-tagged NS1 in 100 μL binding buffer for 30 min at room temperature. One hundred microliters of glutathione agarose beads was added and incubated for another 20 min. The reaction mixture was centrifuged to remove unbound DNA molecules, and pellets were washed 5 times with 500 μL of the binding buffer. The NS1-DNA complex was dissociated from the glutathione agarose beads by eluting with the elution buffer (binding buffer plus 10 mM glutathione). ssDNAs bound to NS1 were recovered from the supernatant by phenol–chloroform extraction and ethanol precipitation. Fifteen sequential selection rounds were repeated using the same procedure. More stringent conditions were employed by reducing the protein concentration from round 8: 1 μg (rounds 8–9), 0.5 μg (rounds 10–11), 0.25 μg (rounds 12–13), and 0.125 μg (rounds 14–15) in 100 μL binding buffer. After the 15th round, ssDNA was amplified by PCR, cloned into a linearized pGEM T vector (Promega), and the DNA sequences were determined as described previously (Cho et al., 2011). Bioinformatics analysis was performed using ClustalW2 and the secondary structures of selected ssDNA aptamers were predicted using the program MFold (Zuker, 1989).

2.2. Measurement of the NS1 protein – ssDNA aptamer interaction by ELISA

5′-Biotinylated aptamers were generated by PCR using a 5′-biotinylated forward primer (5′-Biotin-GCAATGTACGGTACTTCC-3′), followed by λ-exonuclease digestion as described previously (Cho et al., 2011). The 5′-biotinylated ssDNA aptamers were denatured at 90 °C for 10 min, immediately put on ice, added to the wells of a streptavidin-coated plate (Pierce), and incubated for 1 h at room temperature while shaking at 100 rpm. The wells were washed with phosphate buffered saline with Tween (PBST; 0.1% Tween 20 in PBS; pH 7.4) 4 times and blocked with 5% BSA in PBST at room temperature for 1 h to prevent non-specific binding. After washing, various concentrations of purified GST-tagged NS1 protein (100 nM/100 μL in PBS per well) were added to wells and incubated for 1 h at room temperature. The wells were then washed with PBST, and the bound GST-tagged NS1 proteins were detected by incubating with 100 μL of GST antibody-conjugated horseradish peroxidase (HRP) (1:1000 in PBST, Santa Cruz) for 1 h at room temperature. After washing, the color developing reaction was initiated by adding 100 μL of 3,3′,5,5′-Tetrametylbenzidine (TMB) solution (Merck) per well, and terminated by adding 2.5 N H_2SO_4. The absorbance of each well was measured at 450 nm using a TRIAD microplate reader (Dynex Technologies, USA).

To determine which NS1 subdomain was responsible for binding to the selected ssDNA aptamer, enzyme-linked immunosorbent assay (ELISA) experiments were performed as described above with slight modifications. Various types of the NS1 protein (full length, RNA-binding domain, effector domain, K41A mutant, and R38A/K41A mutant) were added to a glutathione-coated plate (100 nM/100 μL in PBS per well), and incubated for 1 h at room temperature while shaking at 100 rpm. Each well was washed with PBST, blocked with BSA in PBST, and incubated with the selected 5′-biotinylated aptamer (100 nM/100 μL in PBS per well) for 1 h at room temperature. After washing, the bound aptamers were detected using a streptavidin-conjugated HRP (1:10,000 in PBST, Pierce) and the color developing reaction was performed as described above.

2.3. Circular dichroism (CD) spectroscopy

ssDNA (25 μM) was resuspended in 10 mM Tris/Cl (pH 7.5) buffer with 100 mM KCl. CD spectra were collected on a Chirascan plus spectrometer (Applied Photophysics, UK) at 200–320 nm, using 3 scans at a step size of 1 nm, a 0.2 s time-per-point, and a bandwidth of 1 nm. All spectra were acquired at room temperature and were buffer baseline corrected.

2.4. Cell culture and viruses

Cells of the human embryonic kidney epithelial cell line HEK293T were cultured in Dulbecco's modified minimal essential medium supplemented with 100 U penicillin and 10% fetal bovine

serum at 37 °C and 5% CO_2. The pcDNA6-AIV NS1 construct was produced by cloning the PCR-amplified NS1 gene of the A/HK/483/97(H5N1) strain (GenBank accession number AF084286) into the *Bam*HI/*Eco*RI sites of pcDNA6/myc-His (Invitrogen). The pcDNA6-AIV NS1 gene was transfected into 293T cells (293T/NS1) using Lipofectamine™ 2000 (Invitrogen), according to the manufacturer's instructions. After 6 h incubation, the medium was replaced by another medium containing 1% (w/v) polyI:C (GE Healthcare, UK) and maintained with 10 μg/mL blasticidin (Invitrogen).

RAW 264.7, a murine macrophage cell line (ATCC TIB–71) was maintained in Dulbecco's Modified Eagles Minimum essential medium (DMEM, Invitrogen, USA) containing 10% fetal bovine serum (FBS) (Gibco, USA) and 1% antibiotic/anti-mycotic (Gibco, USA) at 37 °C with 5% CO_2 until use.

The PR8 strain of Influenza A virus (**A**/Puerto Rico/8/34/H1N1) which is encoded with green fluorescence protein (GFP) was propagated in allantoic fluid of 10-day-old chicken embryos, purified through ultracentrifugation at 28,000 rpm for 3 h using 20% sucrose column, re-suspended in Phosphate Buffered Saline (PBS) and stored at −70 °C until use.

2.5. Confocal imaging

The selected ssDNA aptamer was labeled with fluorescein isothiocyanate (FITC) for confocal imaging. 293T cells harboring NS1 (293T/NS1) in 1% polyI:C medium were transfected with the FITC-labeled ssDNA aptamer using lipofectamin 2000. After a 48-h incubation period, transfected cells were fixed with 4% paraformaldehyde for 10 min, permeabilized with 0.1% (v/v) Triton X-100 for 5 min, blocked with 1% BSA in PBS for 30 min, and incubated with a phycoerythrin (PE)-conjugated anti-6X His-tag antibody (Abcam) in PBS with 1% BSA for 30 min at room temperature. The samples were then briefly reacted with 3 ng/mL 4′,6-Diamidino-2-Phenylindole (DAPI) (Invitrogen) in PBS for 10 min and washed several times with PBS. Confocal microscopy was performed using a Carl Zeiss LSM 700 laser-scanning microscope (Zeiss) fitted with a 40X Axio objective and ZEN imaging software.

2.6. Flow cytometric analysis

To monitor the selectivity of the ssDNA aptamer, 293T/NS1 cells in the absence of polyI:C were harvested with trypsin–EDTA, washed 3 times with 1 mL of PBS, fixed in 4% paraformaldehyde solution, and washed 3 times with 1 mL of PBS. Cells were then permeabilized with 0.1% (v/v) Triton X-100 for 15 min at 4 °C, blocked with 1% BSA in PBS for 15 min, and reacted with 1 μg of the FITC-labeled aptamer in PBS for 30 min at 4 °C. The samples were further incubated with a PE-conjugated anti-6X His-tag antibody (Abcam) in PBS for 30 min at 4 °C and washed several times with PBS. Cells were suspended in 500 μL of PBS with 10% fetal calf serum and 1% NaN_3. The fluorescence was determined with a FACScan Cytometer (BD system) by counting 10,000 events. The FITC-labeled ssDNA library was used as a negative control.

2.7. Luciferase reporter gene assay

To measure the NF-κB activity, a p4xκB-firefly luciferase DNA construct (p4xκB-luc) was kindly provided by Dr. Young-Guen Kwon (Yonsei University, Seoul, Korea) and Renilla luciferase DNA pGL was purchased from Promega. For the luciferase reporter gene assay, 4×10^6 293T cells were plated in a tissue culture dish (10 cm diameter) and the next day they were transfected with 150 ng of p4xκB-luc and 50 ng of pGL using the Fugene HD Transfection Reagent (Roche). After 24 h incubation, cells were detached from the tissue culture dish, plated in a 24-well plate (3×10^3), and then further incubated for 24 h. Subsequently, cells were transfected with 0.8 μg of pcDNA6-AIV NS1 and the indicated amount of aptamers using the Lipofectamine™ 2000 (Invitrogen), according to the manufacturer's instructions. After 6 h incubation, NF-κB was induced by replacement of the medium by another medium containing 1% polyI:C. Luciferase activities were measured after 48 h using the Dual-luciferase Reporter Assay system (Promega). The luminescence of firefly luciferase and Renilla luciferase were measured using the Centro LB 960 luminometer (Berthold), and the firefly luciferase activity was normalized to that of Renilla luciferase.

2.8. Quantitative RT-PCR and interferon-beta ELISA

Total RNA was extracted from cell pellets using easy BLUE solution (Intron, South Korea). Total RNA was dissolved in RNase-free water, and the concentration was determined by measurement of the optical density at 260 nm. cDNA was synthesized from total RNA (1 μg) using the RT premix kit (Intron, South Korea) according to the manufacturer's instructions. Quantitative reverse transcription PCR (qRT-PCR) was performed using reagents provided in SYBR® premixEx Taq™ II (Takara) in the Light cycler® 2.0 (Roche), according to the manufacturer's instructions. RT was performed with oligo dT primers from 1 μg total RNA. PCR primers for the human INF-β and the internal control human β-actin gene were designed using Primer-Blast software (http://www.ncbi.nlm.nih.gov/tools/primer-blast/). The primers used were: INF-β forward primer (5′-CGCCGCATTGACCATCTA-3′), INF-β reverse primer (5′-GACATTAGCCAGGAGGTTCTCA-3′); human-β actin forward primer (5′-GCGAGCACAGAGCCTCGCCT-3′), and human-β actin reverse primer (5′-GCCTTGCACATGCCGGAGCC-3′). Cell culture supernatants were collected and analyzed for IFN-β production using the IFN-β ELISA kit (PBL Biomedical Laboratories), according to the manufacturer's instructions.

2.9. Inhibition of virus replication by NS1 aptamer on RAW 264.7 cells

To evaluate the antiviral effect of NS1 aptamer against Influenza virus infection, the virus replication inhibition was observed as described previously (Moon et al., 2012). In brief, RAW 264.7 cells were cultured (8×10^5/well) onto 12-well plates for 12 h. Then, cells were transfected with different amount of aptamer (0, 100, 200, 400 and 800 ng in 1 ml culture media) using lipofectamin 2000 (Invitrogen, USA), according to manufacturer's protocol. The recombinant mouse interferon-β (Sigma, USA) 1000 units/ml was used as a positive control to compare the effect of treatments.

After 6 h of treatment, the media was substituted by fresh DMEM and cells were infected with PR8–green fluorescent protein (GFP) virus of 1 multiplicity of infection (MOI). Two hours post infection, virus was removed by replacing the media with DMEM containing 10% FBS and further incubated at 37 °C with 5% CO_2. At 12 h post infection, the green fluorescence protein expression was observed using fluorescence microscope at 200× magnification.

To measure the expressed GFP level in each treatment, the cells from each well were collected separately and centrifuged at 1500*g* for 3 min, and the consequential cell pellet was diluted in PBS and transferred to 96-well black plate for GFP detection under the excitation peak wave length of 490 nm using Glomax multi-detection system (Promega, USA). The measured GFP relative units were fit to a hyperbolic decay equation.

3. Results

3.1. In vitro selection of ssDNA aptamers to recognize the NS1 protein of the influenza virus

To discover the ssDNA aptamers, we performed the SELEX procedure, and λ-exonuclease digestion was followed by PCR to generate ssDNA, as shown in Fig. 1A (Cho et al., 2011). Enrichment of ssDNA aptamers specific to NS1 was monitored based on the NS1–biotinylated ssDNA aptamer interaction, and the specific binding activity of the ssDNA pool was measured by ELISA. As shown in Fig. 1B, ssDNA pools isolated after rounds 11–15 were tested for binding affinity and the absorbance at 492 nm increased significantly from round 11. After 15 cycles of selection, we were able to obtain 15 independent ssDNA aptamers, whose sequences were determined. Further measurements of the binding affinity of the 15 selected ssDNA aptamers were performed by ELISA to select the aptamer with the highest binding affinity. The 15 selected ssDNA aptamers were immobilized on streptavidin-coated plates and various concentrations of the NS1 protein were added. After addition of GST-HRP, the absorbance was measured at 450 nm. The binding curve was fit to a hyperbolic equation ($Abs = A[NS1]/(K_d + [NS1]$, where Abs is the absorbance, A is the amplitude, [NS1] is the concentration of NS1, and K_d is the disscociation constant), and the amplitude and K_d value of each ssDNA aptamer were obtained (data not shown). Of the 15 aptamer candidates, the ssDNA aptamer that showed the highest binding affinity for NS1 (K_d = 18.91 ± 3.95 nM) was determined from the binding curve (Fig. 2A). In addition to ELISA, we also performed surface plasmon resonance (SPR) experiments to determine the binding affinity, from which similar binding affinities were obtained (Supplemental Table S1). Based on the determination of binding affinity, the selected ssDNA aptamer was further analyzed bioinformatically. The nucleotide sequence and predicted secondary structure of the aptamer were determined using the MFOLD program (Zuker, 2003) and are shown in Fig. 2B. In this analysis, the 45 nucleotide random sequence region of the selected ssDNA aptamer (shaded nucleotides) was shown to consist of a major loop with 2 hairpins. Interestingly, the aptamer was found to have a characteristic G-rich sequence (73% G) of nucleotides ($GGG(N)_xGGG$), in which is a deoxynucleotide and x is the number of repeats in the 45 nucleotide random sequence region (Fig. 3A). Furthermore, the G-rich sequence was found to be located at the hairpin regions as well as at the large major loop. These analyses indicated that the G-rich sequence might be responsible for the interaction with the NS1 protein. We further analyzed the G-rich sequence biophysically, using circular dichroism, to determine whether the selected aptamer has a G-quadruplex structure since the repeat pattern of $GGG(N)_xGGG$ is likely to form such a structure. Fig. 3B shows 2 CD spectra of the starting ssDNA library (negative control) and the selected aptamer. The ssDNA library showed a positive peak at 280 nm, which is a typical characteristic of normal DNA (Fukuda et al., 2005). On the other hand, the selected aptamer folded into a parallel G-quadruplex structure that was identified by a positive maximum peak at 266 nm and a negative minimum peak at 244 nm (Hardin et al., 1992).

3.2. RNA-binding domain of NS1 is critical for ssDNA aptamer binding

Since NS1 consists of 2 distinct functional domains (Chien et al., 2004; Hatada et al., 1992; Wang et al., 2002), including an N-terminal RNA-binding domain (1–73 amino acids) and an effector domain (74–230), we prepared 5 truncated/mutant proteins to more finely map the ssDNA aptamer-binding domain of the NS1:

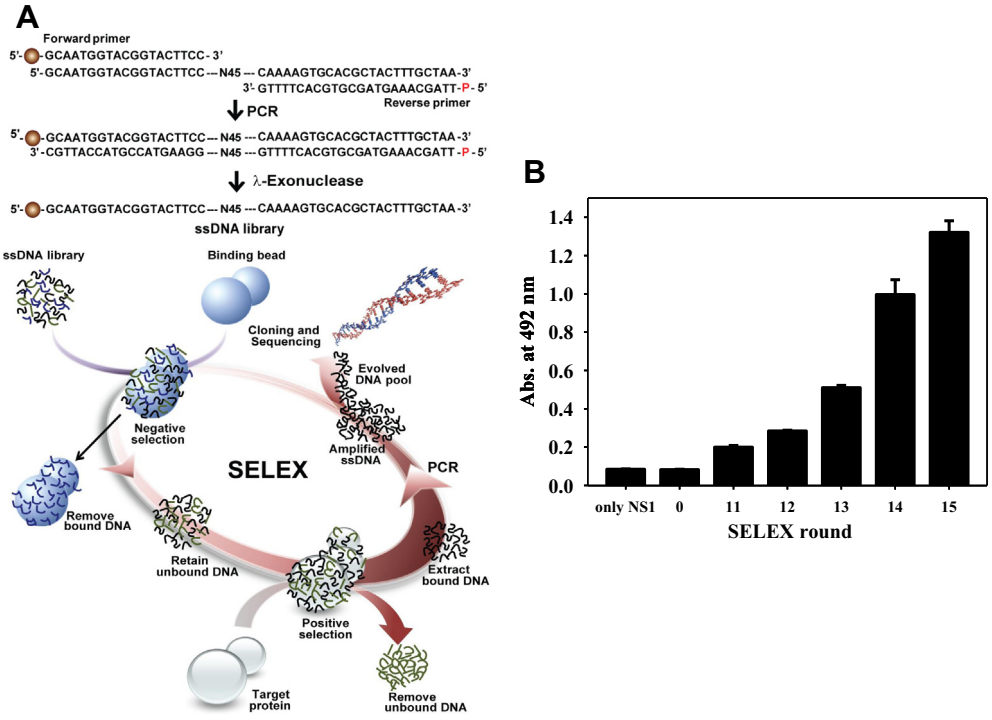

Fig. 1. *In vitro* selection of the ssDNA aptamer and specific binding activity of the ssDNA pool after 15 rounds of selection. (A) Schematic representation of the SELEX procedure. A random ssDNA library was prepared by PCR and λ-exonuclease digestion. Forward and reverse primers have FAM™ (ball symbol) and phosphorylated nucleotides at their 5′-ends, respectively. After removing non-specific binding to glutathione agarose beads, the ssDNA pool was mixed with the GST-tagged NS1 protein. The DNA library bound to the target protein was eluted and amplified using PCR. The DNA was enriched after 15 rounds of selection, and the selected DNA was PCR-amplified, cloned and sequenced. (B) Specific binding affinity was measured by ELISA. After 10 rounds of SELEX, the selected biotin labeled-DNA library was incubated on the target protein-coated plate and then measured using a streptavidin-HRP antibody with TMB solution.

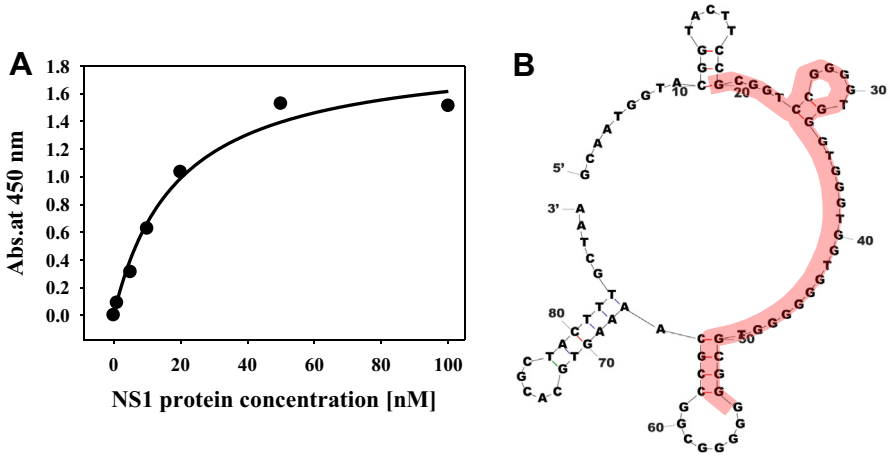

Fig. 2. Affinity measurements of the selected ssDNA aptamer and predicted secondary structure. (A) Affinity measurement of the selected aptamer specific to NS1 by ELISA. The immobilized 5′-biotinylated aptamer was incubated with increasing concentrations of GST-tagged NS1. After addition of GST antibody-conjugated HRP, the amount of the NS1-aptamer complex was calculated and graphed as a function of NS1 concentration. The graph was fit to the Michaelis–Menten equation and the K_d was calculated (18.91 ± 3.95 nM). (B) Predicted secondary structure of the selected ssDNA aptamer using Zuker's MFOLD program. Shaded nucleotides show the 45 random sequence region of the selected aptamer.

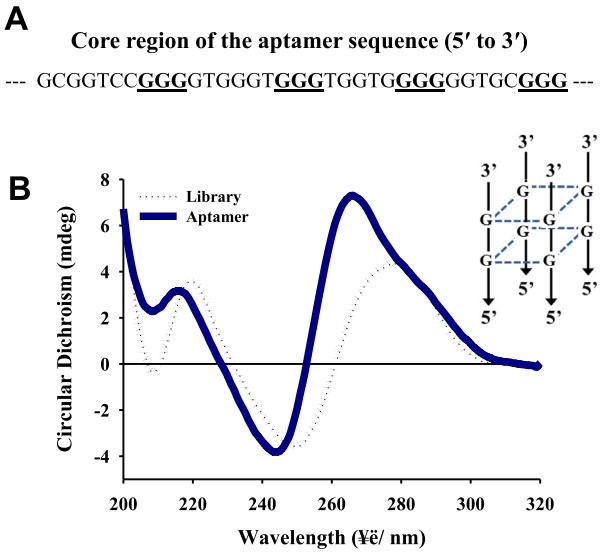

Fig. 3. G-rich sequence of the core region and CD spectra of the selected ssDNA aptamer. (A) G nucleotides of the random sequence region involved in the formation of the G-quadruplex structure as predicted by the QGRS mapper are underlined and are in bold face. (B) CD spectrometry was performed using the starting ssDNA library (dotted line) and the selected ssDNA aptamer (solid line).

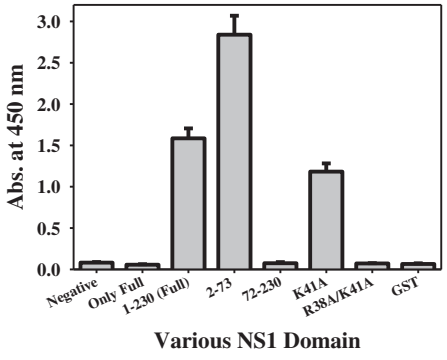

Fig. 4. Affinity measurements of truncated and mutant NS1 using the selected aptamer by ELISA. The immobilized GST-tagged truncated and mutant NS1 was incubated with a 5′-biotinylated aptamer. After addition of streptavidin-HRP, the amount of the NS1-aptamer complex was measured by ELISA. Lane 1, without NS1 and aptamer; Lane 2, full-length NS1 without aptamer; Lane 3, amino acids 1–230 (full-length NS1); Lane 4, amino acids 2–73 (RNA-binding domain); Lane 5, amino acids 72–230 (effector domain); Lane 6, K41A mutant; Lane 7, R38A/K41A double mutant; Lane 8, GST only for a negative control.

amino acids 1–230 (full length), amino acids 2–73 (RNA-binding domain), amino acids 72–230 (effector domain), K41A mutant, and R38A/K41A double mutant. For the 2 mutant proteins, R38 and K41, the conserved basic amino acids are known to be directly required for RNA binding to NS1 and for IFN antagonism (Donelan et al., 2003; Talon et al., 2000b). To determine which subdomain of NS1 is critical for aptamer binding, we performed ELISA experiments by adding a 5′-biotinylated aptamer to immobilized proteins. Fig. 4 shows that the RNA-binding domain is critical for aptamer binding. The RNA-binding domain showed a higher absorbance value compared to that of the full-length NS1, indicating that the selected aptamer binds to the RNA-binding domain rather than to the effector domain. No significant absorbance was observed with the effector domain. Interestingly, the K41A mutant showed absorbance values similar to those of the full-length NS1. However, the R38A/K41A double mutant did not show any significantly detectable binding to the aptamer. Binding affinities of truncated/mutant proteins were also measured by SPR and ELISA methods, as summarized in Supplemental Table S1. Neither Effector domain nor R38A/K41A double mutant showed any binding to the aptamer.

3.3. The selected aptamer binds to NS1 in cells

To better detect the binding ability of the selected aptamer to NS1, confocal microscopy (Fig. 5A) and flow cytometric analysis (Fig. 5B) were performed. To obtain the confocal imaging, 293T/NS1 cells were fixed on the cover glass after transfection of the FITC-labeled aptamer. Fig. 5A shows the distribution of the NS1 protein (red color), the ssDNA aptamers (green color) and the nucleus (blue color stained with DAPI), which were visualized by confocal microscopy. Whereas the cells treated with the negative control ssDNA library did not show any detectable FITC-labeled

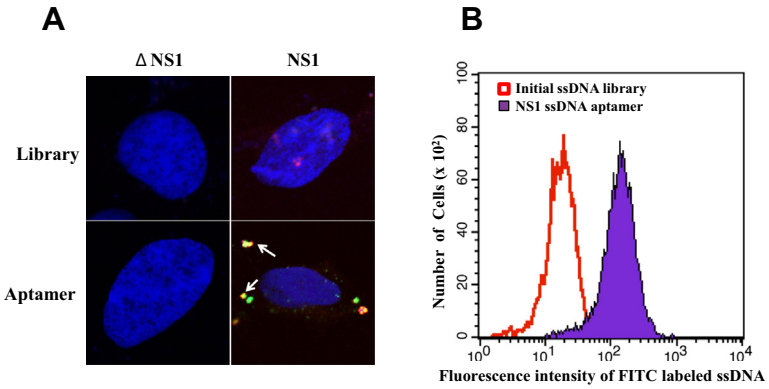

Fig. 5. The selected ssDNA aptamer binding to NS1 protein in cells. (A) 293T only (ΔNS1) and 293T/NS1 cells were transfected with the starting ssDNA library as a negative control (upper panel) and the selected FITC-labeled ssDNA aptamer (lower panel), respectively. Cells were visualized by confocal imaging and the distribution of NS1 (red color by PE conjugated anti-6X His-tag antibody), the selected aptamer (green color by FITC) and the nucleus (blue color stained with DAPI) are shown. Arrows indicate the localization of the FITC-labeled ssDNA aptamer bound to NS1. (B) 293T/NS1 cells were incubated with the FITC-labeled starting ssDNA library as a negative control and the selected FITC-labeled ssDNA aptamer. Binding of the FITC-labeled ssDNA aptamer to NS1 was measured by flow cytometry (shaded area).

DNA binding to NS1 (upper panel), we were able to detect signals of the selected FITC-labeled ssDNA aptamer binding to NS1 (bottom panel). Interestingly, the FITC-labeled aptamer bound to NS1 (orange color, combination of the overlapping red (NS1) and green (aptamer)) was found to be localized in the cytoplasm as granular forms (shown by arrows).

We also investigated whether the selected aptamer specifically binds to NS1, using flow cytometric analysis. As shown in Fig. 5B, while the starting ssDNA library did not bind to NS1, the selected FITC-labeled aptamer showed a significant increase of the fluorescence signal (more than 65%) in 293T/NS1 cells. Taken together, these results indicate that the selected aptamer binds specifically to the target NS1 protein.

3.4. Suppression of interferon antagonism by the ssDNA aptamer

We hypothesized that the selected ssDNA aptamer specific to NS1 inhibits the function of NS1 by binding, thereby promoting the induction of IFN. To test this hypothesis, we employed the cell based IFN-β luciferase reporter assay. When luciferase activities were determined in the presence of the aptamer, IFN-β mediated NF-κB transcriptional activity was augmented as the amount of the selected aptamer increased (Fig. 6A). However, the luciferase activity of 293T cells overexpressing NS1 (MOCK) was very low, demonstrating that overexpressed NS1 plays an antagonistic role on IFN-β expression in cells. Therefore, the selected ssDNA aptamer can be bound to and inhibit the function of NS1. In addition, a quantitative RT-PCR experiment was carried out to measure the mRNA expression level of IFN. After 293T cells were transfected with an NS1 expression vector, along with various amounts of the selected aptamer, cDNA was synthesized from the cell lysate and quantitated. Similar to the results of the luciferase reporter assay, the level of IFN-β mRNA expression increased as the amount of the selected aptamer increased (Fig. 6B). As an alternative attempt to measure IFN-β induction, we performed ELISA experiments to quantitate IFN-β production in cells 48 h posttransfection. Fig. 6C shows that the ELISA result is consistent with the luciferase and qRT-PCR assays as IFN-β production increased as the amount of the selected aptamer increased. Taken together, these results demonstrate that our selected ssDNA aptamer specifically binds to and blocks the function of the NS1 protein, which acts as an agonist of IFN-β production.

3.5. Inhibition of influenza virus replication by the ssDNA aptamer

To determine the effect of the selected aptamer on viral replication, cells were treated with increasing amount of the aptamer for 6 h prior to viral infection, followed by fluorescence analysis. As shown in Fig. 7, viral replication was inhibited significantly even in the presence of 100 ng of aptamer compared to 0 ng treated (approximately one-third of fluorescence unit). When the cells were treated with 800 ng of aptamer, the fluorescence level was almost similar to a positive control (IFN-β). The GFP relative unit decreased in a hyperbolic manner with increasing aptamer concentrations providing a 50% inhibitory concentration of 27.68 ± 6.02 ng/ml (which is equivqlent to 0.99 ± 0.17 nM). However, cytotoxicity was not observed regardless of the amount of treated aptamer (Supplemental Fig. S1).

4. Discussion

Viruses have evolved mechanisms to evade their host's antiviral responses, and virus-encoded IFN antagonists play a major role in the suppression of host innate immunity (Garcia-Sastre and Biron, 2006; Haller et al., 2006). Influenza also has an IFN antagonist, NS1, which has been shown to prevent the activation of IRF-3 and NF-κB, among others, thereby inhibiting IFN induction (Ludwig et al., 2002; Talon et al., 2000a). Therefore, inhibition of NS1 function may attenuate and/or limit further viral infection in the host cells by activation of IFN induction. In fact, it has been demonstrated that NS1 is a good target protein for the development of an antiviral agent in cell culture and animal model system (Basu et al., 2009; Garaigorta et al., 2005; Garcia-Sastre et al., 1998; Jackson et al., 2008). In the present study, ssDNA aptamer was suggested as a novel NS1 antagonist and investigated a potential usefulness for treatment of influenza. We constructed an 88mer ssDNA pool containing a randomized sequence region of 45 nucleotides in the center, which was screened in order to isolate ssDNA aptamers specific to the NS1 protein. The selected aptamer was structurally investigated and found to have a G-quadruplex structure by CD. Although several aptamers that have a G-quadruplex structure similar to that observed in the present study have been reported, their exact binding mode to target proteins remains unknown (Vairamani and Gross, 2003; Weiss et al., 1997).

Further investigation to determine the aptamer binding region of NS1 revealed that RBD is critical. Although the reason why the

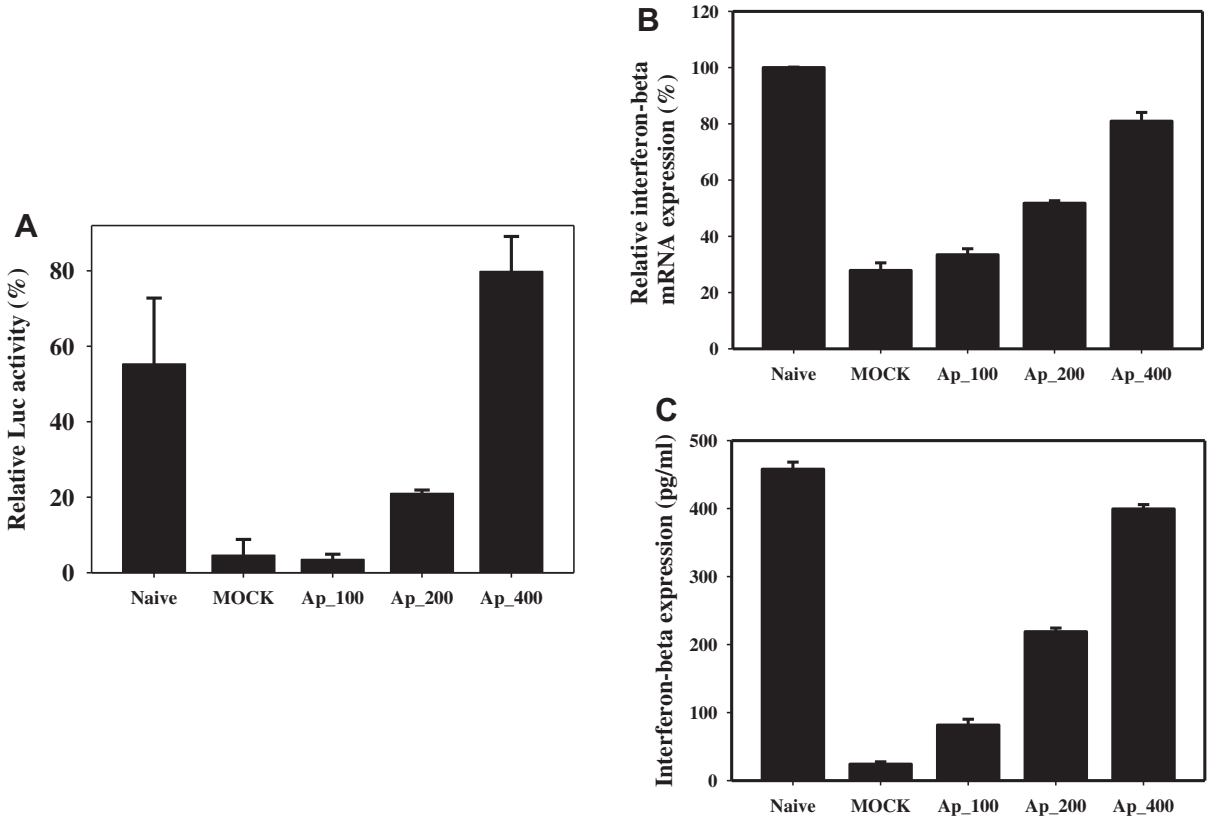

Fig. 6. IFN-β induction in cells by suppression of NS1. (A) Luciferase gene reporter assay was performed as described in Section 2 with various amounts of the selected aptamer (0, 100, 200 and 400 ng). (B) Quantitative RT-PCR was carried out to quantitate the production of IFN-β mRNA with various amounts of the selected aptamer. (C) The levels of expressed IFN-β were measured with various amounts of the selected aptamer by ELISA. The data represents average values after 3 independent experiments. Naïve; 293T cells only (ΔNS1), MOCK; 293T/NS1 cells, Ap_100, 200 and 400; 293T/NS1 cells transfected with 100, 200 and 400 ng of the selected ssDNA aptamer, respectively.

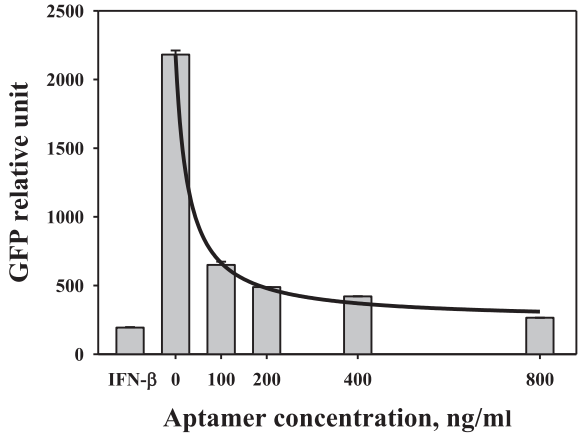

Fig. 7. Suppression of viral propagation by the selected aptamer. RAW264.7 cells were transfected with different amount of aptamer (0, 100, 200, 400 and 800 ng in 1 ml culture media) using lipofectamin 2000. After 6 h treatment, cells were infected with PR8–GFP virus of 1 multiplicity of infection (MOI). Fluorescence signals were detected using Glomax multi-detection system. The recombinant mouse IFN-β 1000 units/ml was used as a positive control (lane INF- β) to compare the effect of treatments. The GFP relative unit *versus* [aptamer] fit to a hyperbolic decay equation with a 50% inhibitory concentration of 27.68 ± 6.02 ng/ml (which is equivalent to 0.99 ± 0.17 nM).

absorbance of the RNA-binding domain was higher than that of the full-length NS1 is not clear, it is likely that the RNA-binding domain without the effector domain is more accessible to the aptamer than is the full-length domain from a structural perspective. Moreover, ELISA experiments with two mutant proteins (K41A and R38A/K41A) were also performed because the two amino acids are important for RNA binding to NS1. Similar to previous reports, the exact binding mode of the selected aptamer is not known at present, if these 2 amino acid residues are involved in the binding, the aptamer will nonetheless be useful for future studies involving RNA binding and innate immune responses. Our results showed that R38A/K41A did not bind to the selected aptamer. This suggests that the R38 residue is required for aptamer binding in NS1. The three-dimensional structure of each domain has been reported for a few influenza virus strains (Bornholdt and Prasad, 2006; Chien et al., 1997; Hale et al., 2008; Liu et al., 1997); however, the structure of the full-length NS1 has yet to be determined. Therefore, further study will be necessary in order to determine precisely how the R38 residue is involved in aptamer binding.

According to a previous study, TRIM25 overexpression can affect the subcellular localization of NS1 from the nucleus to the cytoplasm (Gack et al., 2009). In addition, the cellular localization of RIG-I infected with NS1-deficient IAV, which is known to interact with TRIM25, has been shown to exhibit a speckle-like distribution in the cytoplasm (Onomoto et al., 2012). Under our experimental conditions, polyI:C binding to RIG-I was assumed to trigger the formation of speckle-like antiviral stress granules, which contain RIG-I, other antiviral proteins, and polyI:C. Therefore, the localization of NS1 and the bound FITC-labeled aptamer (the dots designated by arrows in Fig. 5A) are consistent with results of recent studies on the localization of RIG-I and NS1. The confocal images in the present study also indicate that the selected aptamer efficiently blocks NS1 function, thereby enabling the RIG-I to form speckle-like granules.

It is also assumed that the selected aptamer would bind through NS1's antibody-binding domain. When we used NS1 primary antibody and dye labeled secondary antibody instead of the PE conjugated anti-6X His-tag antibody, the signal strength of the confocal image was not significant (data not shown). This implied that the selected aptamer, which was bound to the antibody-binding domain of NS1, prevented the NS1 primary antibody from binding to NS1. In contrast, the PE conjugated anti-6X His-tag antibody had no obstacles in binding to NS1, thus enabling the detection of better signals.

Subsequent studies revealed that the selected aptamer was successfully able to induce IFN and block the viral replication (Fig. 6 and Fig. 7). This implies that simply inhibiting the function of NS1 is great helpful to overcome the viral infection. In fact, many attempts have been made to find potential small molecules against NS1 (Basu et al., 2009; Jablonski et al., 2012; Walkiewicz et al., 2011). Based on recent progress of nucleic acid aptamer, we thought ssDNA aptamer might be another good candidate to inhibit the function of NS1 and restore innate immunity. Although we propose that ssDNA aptamer specific to NS1 has a good potential to be developed as a therapeutic agent in this study, we would like to point out a few limitations. We investigated only one NS1 gene, so that more intensive studies on the protein interactions with NS1, such as interaction with RIG-I, will be necessary for the selected aptamer to be a therapeutic agent. We are going to perform experiments to see if the selected aptamer inhibits the interaction of NS1 with RIG-I through *in vitro* and cell-based assay. We also think that resistance to nuclease attack through base/sugar modification and PEGylation should be included in the future study to improve the efficiency of the selected aptamer. Regarding the issues related to *in vivo* applications, studies on the efficient delivery of aptamer into cells and timing of treatment post-infection should be necessary. And we think the selected aptamer is unsuitable in case of immunocompromised patients. However we showed strong potentials of the aptamer to inhibit the viral replication in this study despite of a few limitations. We expect our aptamer to be developed as a therapeutic agent after careful modifications.

5. Conclusions

In this study, we isolated an ssDNA aptamer specific to the IAV NS1 protein using the SELEX procedure. The strength of the binding was in the low nanomolar range, and the selected ssDNA aptamer showed effective and specific binding to NS1. Bioinformatics analysis further showed that the selected aptamer has a G-quadruplex structure, although the precise binding mode is not known in detail. Because IAV NS1 is an important antagonist of IFN-β induction, we further investigated the selected aptamer as a potential candidate as an antiviral agent. Interestingly, we observed significant recovery of IFN induction as the amount of the aptamer increased, strongly suggesting that the selected aptamer efficiently inhibits the function of NS1. Further studies with virus infected cells revealed that the selected aptamer was able to inhibit the viral replication, indicating restoration of IFN induction by the aptamer leads to block the propagation of virus. An RNA aptamer may provide better structural diversity and be more widely used to block the function of target proteins. However, unmodified RNA is labile, susceptible to nuclease, and is easily destroyed under physiological conditions. For these reasons, we decided to develop a DNA, rather than RNA, aptamer in the present study. Future studies will be necessary to improve the stability of the selected ssDNA aptamer, including base modification of nucleotides, capping of DNA fragments, and end labeling with appropriate chemicals that act against nuclease attack (Shum and Tanner, 2008).

Acknowledgements

This study was supported by a Grant of the Korea Healthcare technology R&D Project, Ministry of Health & Welfare, Republic of Korea. (Grant No.: A103001) We declared no conflict of interest.

Appendix A. Supplementary data

Supplementary data associated with this article can be found, in the online version, at http://dx.doi.org/10.1016/j.antiviral.2013.09.004.

References

Basu, D., Walkiewicz, M.P., Frieman, M., Baric, R.S., Auble, D.T., Engel, D.A., 2009. Novel influenza virus NS1 antagonists block replication and restore innate immune function. J. Virol. 83, 1881–1891.
Bornholdt, Z.A., Prasad, B.V., 2006. X-ray structure of influenza virus NS1 effector domain. Nat. Struct. Mol. Biol. 13, 559–560.
Brody, E.N., Gold, L., 2000. Aptamers as therapeutic and diagnostic agents. J. Biotechnol. 74, 5–13.
Bunka, D.H., Platonova, O., Stockley, P.G., 2010. Development of aptamer therapeutics. Curr. Opin. Pharmacol. 10, 557–562.
Cheng, C., Dong, J., Yao, L., Chen, A., Jia, R., Huan, L., Guo, J., Shu, Y., Zhang, Z., 2008. Potent inhibition of human influenza H5N1 virus by oligonucleotides derived by SELEX. Biochem. Biophys. Res. Commun. 366, 670–674.
Chien, C.Y., Tejero, R., Huang, Y., Zimmerman, D.E., Rios, C.B., Krug, R.M., Montelione, G.T., 1997. A novel RNA-binding motif in influenza A virus non-structural protein 1. Nat. Struct. Biol. 4, 891–895.
Chien, C.Y., Xu, Y., Xiao, R., Aramini, J.M., Sahasrabudhe, P.V., Krug, R.M., Montelione, G.T., 2004. Biophysical characterization of the complex between double-stranded RNA and the N-terminal domain of the NS1 protein from influenza A virus: evidence for a novel RNA-binding mode. Biochemistry 43, 1950–1962.
Cho, S.J., Woo, H.M., Kim, K.S., Oh, J.W., Jeong, Y.J., 2011. Novel system for detecting SARS coronavirus nucleocapsid protein using an ssDNA aptamer. J. Biosci. Bioeng. 112, 535–540.
Donelan, N.R., Basler, C.F., Garcia-Sastre, A., 2003. A recombinant influenza A virus expressing an RNA-binding-defective NS1 protein induces high levels of beta interferon and is attenuated in mice. J. Virol. 77, 13257–13266.
Egorov, A., Brandt, S., Sereinig, S., Romanova, J., Ferko, B., Katinger, D., Grassauer, A., Alexandrova, G., Katinger, H., Muster, T., 1998. Transfectant influenza A viruses with long deletions in the NS1 protein grow efficiently in Vero cells. J. Virol. 72, 6437–6441.
Fukuda, H., Katahira, M., Tanaka, E., Enokizono, Y., Tsuchiya, N., Higuchi, K., Nagao, M., Nakagama, H., 2005. Unfolding of higher DNA structures formed by the d(CGG) triplet repeat by UP1 protein. Genes Cells 10, 953–962.
Gack, M.U., Albrecht, R.A., Urano, T., Inn, K.S., Huang, I.C., Carnero, E., Farzan, M., Inoue, S., Jung, J.U., Garcia-Sastre, A., 2009. Influenza A virus NS1 targets the ubiquitin ligase TRIM25 to evade recognition by the host viral RNA sensor RIG-I. Cell Host Microbe 5, 439–449.
Garaigorta, U., Falcon, A.M., Ortin, J., 2005. Genetic analysis of influenza virus NS1 gene: a temperature-sensitive mutant shows defective formation of virus particles. J. Virol. 79, 15246–15257.
Garcia-Sastre, A., Biron, C.A., 2006. Type 1 interferons and the virus-host relationship: a lesson in detente. Science 312, 879–882.
Garcia-Sastre, A., Egorov, A., Matassov, D., Brandt, S., Levy, D.E., Durbin, J.E., Palese, P., Muster, T., 1998. Influenza A virus lacking the NS1 gene replicates in interferon-deficient systems. Virology 252, 324–330.
Grimm, D., Staeheli, P., Hufbauer, M., Koerner, I., Martinez-Sobrido, L., Solorzano, A., Garcia-Sastre, A., Haller, O., Kochs, G., 2007. Replication fitness determines high virulence of influenza A virus in mice carrying functional Mx1 resistance gene. Proc. Natl. Acad. Sci. USA 104, 6806–6811.
Guo, Z., Chen, L.M., Zeng, H., Gomez, J.A., Plowden, J., Fujita, T., Katz, J.M., Donis, R.O., Sambhara, S., 2007. NS1 protein of influenza A virus inhibits the function of intracytoplasmic pathogen sensor, RIG-I. Am. J. Respir. Cell Mol. Biol. 36, 263–269.
Hale, B.G., Randall, R.E., Ortin, J., Jackson, D., 2008. The multifunctional NS1 protein of influenza A viruses. J. Gen. Virol. 89, 2359–2376.
Haller, O., Kochs, G., Weber, F., 2006. The interferon response circuit: induction and suppression by pathogenic viruses. Virology 344, 119–130.
Hardin, C.C., Watson, T., Corregan, M., Bailey, C., 1992. Cation-dependent transition between the quadruplex and Watson–Crick hairpin forms of d(CGCG3GCG). Biochemistry 31, 833–841.
Hatada, E., Takizawa, T., Fukuda, R., 1992. Specific binding of influenza A virus NS1 protein to the virus minus-sense RNA in vitro. J. Gen. Virol. 73 (Pt 1), 17–25.
Jablonski, J.J., Basu, D., Engel, D.A., Geysen, H.M., 2012. Design, synthesis, and evaluation of novel small molecule inhibitors of the influenza virus protein NS1. Bioorg. Med. Chem. 20, 487–497.
Jackson, D., Hossain, M.J., Hickman, D., Perez, D.R., Lamb, R.A., 2008. A new influenza virus virulence determinant: the NS1 protein four C-terminal residues modulate pathogenicity. Proc. Natl. Acad. Sci. USA 105, 4381–4386.

Kaisho, T., Akira, S., 2006. Toll-like receptor function and signaling. J. Allergy Clin. Immunol. 117, 979–987.
Kochs, G., Koerner, I., Thiel, L., Kothlow, S., Kaspers, B., Ruggli, N., Summerfield, A., Pavlovic, J., Stech, J., Staeheli, P., 2007. Properties of H7N7 influenza A virus strain SC35M lacking interferon antagonist NS1 in mice and chickens. J. Gen. Virol. 88, 1403–1409.
Kurokawa, M., Koyama, A.H., Yasuoka, S., Adachi, A., 1999. Influenza virus overcomes apoptosis by rapid multiplication. Int. J. Mol. Med. 3, 527–530.
Liu, J., Lynch, P.A., Chien, C.Y., Montelione, G.T., Krug, R.M., Berman, H.M., 1997. Crystal structure of the unique RNA-binding domain of the influenza virus NS1 protein. Nat. Struct. Biol. 4, 896–899.
Ludwig, S., Wang, X., Ehrhardt, C., Zheng, H., Donelan, N., Planz, O., Pleschka, S., Garcia-Sastre, A., Heins, G., Wolff, T., 2002. The influenza A virus NS1 protein inhibits activation of Jun N-terminal kinase and AP-1 transcription factors. J. Virol. 76, 11166–11171.
Moon, H.J., Lee, J.S., Choi, Y.K., Park, J.Y., Talactac, M.R., Chowdhury, M.Y., Poo, H., Sung, M.H., Lee, J.H., Jung, J.U., Kim, C.J., 2012. Induction of type I interferon by high-molecular poly-gamma-glutamate protects B6.A2G-Mx1 mice against influenza A virus. Antiviral Res. 94, 98–102.
Onomoto, K., Jogi, M., Yoo, J.S., Narita, R., Morimoto, S., Takemura, A., Sambhara, S., Kawaguchi, A., Osari, S., Nagata, K., Matsumiya, T., Namiki, H., Yoneyama, M., Fujita, T., 2012. Critical role of an antiviral stress granule containing RIG-I and PKR in viral detection and innate immunity. PLoS ONE 7, e43031.
Pichlmair, A., Schulz, O., Tan, C.P., Naslund, T.I., Liljestrom, P., Weber, F., Reis e Sousa, C., 2006. RIG-I-mediated antiviral responses to single-stranded RNA bearing 5′-phosphates. Science 314, 997–1001.
Randall, R.E., Goodbourn, S., 2008. Interferons and viruses: an interplay between induction, signalling, antiviral responses and virus countermeasures. J. Gen. Virol. 89, 1–47.
Shum, K.T., Tanner, J.A., 2008. Differential inhibitory activities and stabilisation of DNA aptamers against the SARS coronavirus helicase. ChemBioChem 9, 3037–3045.
Suarez, D.L., Perdue, M.L., 1998. Multiple alignment comparison of the non-structural genes of influenza A viruses. Virus Res. 54, 59–69.
Talon, J., Horvath, C.M., Polley, R., Basler, C.F., Muster, T., Palese, P., Garcia-Sastre, A., 2000a. Activation of interferon regulatory factor 3 is inhibited by the influenza A virus NS1 protein. J. Virol. 74, 7989–7996.
Talon, J., Salvatore, M., O'Neill, R.E., Nakaya, Y., Zheng, H., Muster, T., Garcia-Sastre, A., Palese, P., 2000b. Influenza A and B viruses expressing altered NS1 proteins: a vaccine approach. Proc. Natl. Acad. Sci. USA 97, 4309–4314.
Twu, K.Y., Noah, D.L., Rao, P., Kuo, R.L., Krug, R.M., 2006. The CPSF30 binding site on the NS1A protein of influenza A virus is a potential antiviral target. J. Virol. 80, 3957–3965.
Vairamani, M., Gross, M.L., 2003. G-quadruplex formation of thrombin-binding aptamer detected by electrospray ionization mass spectrometry. J. Am. Chem. Soc. 125, 42–43.
Vo, N.V., Oh, J.W., Lai, M.M., 2003. Identification of RNA ligands that bind hepatitis C virus polymerase selectively and inhibit its RNA synthesis from the natural viral RNA templates. Virology 307, 301–316.
Walkiewicz, M.P., Basu, D., Jablonski, J.J., Geysen, H.M., Engel, D.A., 2011. Novel inhibitor of influenza non-structural protein 1 blocks multi-cycle replication in an RNase L-dependent manner. J. Gen. Virol. 92, 60–70.
Wang, X., Li, M., Zheng, H., Muster, T., Palese, P., Beg, A.A., Garcia-Sastre, A., 2000. Influenza A virus NS1 protein prevents activation of NF-kappaB and induction of alpha/beta interferon. J. Virol. 74, 11566–11573.
Wang, X., Basler, C.F., Williams, B.R., Silverman, R.H., Palese, P., Garcia-Sastre, A., 2002. Functional replacement of the carboxy-terminal two-thirds of the influenza A virus NS1 protein with short heterologous dimerization domains. J. Virol. 76, 12951–12962.
Weiss, S., Proske, D., Neumann, M., Groschup, M.H., Kretzschmar, H.A., Famulok, M., Winnacker, E.L., 1997. RNA aptamers specifically interact with the prion protein PrP. J. Virol. 71, 8790–8797.
Yoneyama, M., Kikuchi, M., Natsukawa, T., Shinobu, N., Imaizumi, T., Miyagishi, M., Taira, K., Akira, S., Fujita, T., 2004. The RNA helicase RIG-I has an essential function in double-stranded RNA-induced innate antiviral responses. Nat. Immunol. 5, 730–737.
Zuker, M., 1989. Computer prediction of RNA structure. Methods Enzymol. 180, 262–288.
Zuker, M., 2003. Mfold web server for nucleic acid folding and hybridization prediction. Nucleic Acids Res. 31, 3406–3415.